



1 **Climate and Cryosphere Cause Regime Shifts in Water**
2 **Yield over the Upper Brahmaputra River**

3 Hao Li¹, Liu Liu², Baoying Shan³, Lei Wang⁴, Akash Koppa¹, Feng Zhong⁵, Dongfeng Li⁶,
4 Xuanxuan Wang², Wenfeng Liu², Xiuping Li⁴, and Zongxue Xu⁷

5 ¹Hydro-Climate Extremes Lab, Ghent University, Ghent, Belgium

6 ²Center for Agricultural Water Research in China, China Agricultural University, Beijing, China

7 ³Research Unit Knowledge-based Systems, Ghent University, Ghent, Belgium

8 ⁴Institute of Tibetan Plateau Research, Chinese Academy of China, Beijing, China

9 ⁵College of Hydrology and Water Resources, Hohai University, Nanjing, China

10 ⁶Department of Geography, National University of Singapore, Singapore

11 ⁷College of Water Sciences, Beijing Normal University, Beijing, China

12 *Correspondence to:* Liu Liu (liuliu@cau.edu.cn)



13 **Abstract.** Although evidence of hydrological responses to climate is abundant, changes in water yield (WY)
14 in mountainous regions due to climate change and intensified cryospheric melt remain unclear, mainly
15 because of limited observations and large uncertainties in cryosphere-hydrological modeling. In this study,
16 we used annual runoff observations and a high-resolution precipitation dataset to examine the long-term
17 changes in WY in the Upper Brahmaputra River (UBR) basin, as represented by six sub-basins from the
18 stream head to downstream. We found that WY generally increased during 1982–2013, but regime shifts
19 were detected in the late 1990s. Moreover, the direction of the changes in WY reversed from increasing to
20 decreasing in recent years despite the magnitude of the changes continually increasing from less than 10% to
21 80.5%. Furthermore, we used the double mass curve technique to assess the effects of climate, vegetation,
22 and the cryosphere on WY. The results showed that the climate and cryosphere together contributed to over
23 80% of the magnitude increases in WY over the entire UBR basin. However, the combined effects were
24 either offsetting or additive, further leading to slight or substantial magnitude increases, respectively, in
25 which the role of vegetation was nearly negligible. Nevertheless, we found that meltwater from the
26 cryosphere had the potential to alleviate the loss of water availability, which mainly resulted from reduced
27 effective precipitation in most regions. Therefore, the combined effects of climate and cryosphere changes
28 should be considered in ecological restoration and water resources management, particularly involving co-
29 benefits for upstream and downstream regions.



30 **1 Introduction**

31 Water yield (WY) in mountains is crucial for sustaining fragile ecosystems in the headwaters, supplying
32 valuable freshwater resources to downstream lowlands, and balancing co-benefits between the upstream
33 and downstream areas, especially for large transboundary river systems (Viviroli et al., 2011). In
34 mountainous regions, changes in WY have been commonly, but separately, attributed to climate changes
35 (Dierauer et al., 2018; Song et al., 2021), vegetation (Goulden and Bales, 2014; Zhou et al., 2021), and the
36 cryosphere (such as glacial snow melt; see Kraaijenbrink et al. 2021). These changes are expected to alter
37 the spatial and temporal distribution of water resources (Tang et al., 2019) and further threaten the water
38 supply and food security downstream (Biemans et al., 2019). Despite some in situ observations and runoff
39 estimates from state-of-the-art remote sensing technology, the total river runoff for the Third Pole, which is
40 also known as the “Asian Water Tower,” has never been reliably quantified, and its responses to climate
41 change remain unclear (Wang L et al., 2021). Therefore, comprehensively assessing the impacts of the
42 climate, vegetation, and cryosphere on long-term changes, particularly in magnitude and direction, in WY
43 in this region is of great importance for the sustainable development of water resources and ecological
44 environment (Yao et al., 2019).

45 The Qinghai-Tibet Plateau (QTP), regarded as the center of the Third Pole, is one of the most
46 sensitive and vulnerable mountainous regions to environmental changes (Kang et al., 2010; Yao et al.,
47 2010, 2019) and supplies water resources for major rivers in Asia, such as Brahmaputra, Salween, Mekong,
48 Yangtze, Yellow, and Indus Rivers. Changes in WY in this region are a crucial factor in the use of water
49 resources, prevention of natural disasters, and protection of aquatic functions for the livelihoods of
50 approximately two billion people in the area (Immerzeel et al., 2010). In recent years, changes in the
51 climate, vegetation, and cryosphere have significantly affected the WY over the QTP (Bibi et al., 2018).
52 For example, Fan and He (2015) highlighted the effects of precipitation on the direction of change in WY
53 over the Salween and Mekong River basins. Li et al. (2020) determined that elevated precipitation and
54 warming-induced changes in glacial snow patterns both contributed to the magnitude of the increase in
55 WY for the Tuotuo River (a headwater of the Yangtze River). Similarly, Lutz et al. (2014) projected that
56 increased precipitation near the Salween and Mekong Rivers and accelerated meltwater near the Indus
57 River caused major changes in WY. Moreover, the role of vegetation in mountain water resources is
58 important. Li et al. (2017) showed that increased evapotranspiration, mostly due to grassland restoration,
59 decreased the WY in the Yangtze River basin, while Li et al. (2021) suggested that vegetation greening
60 was mainly linked to the positive WY trend during the dry season over the Brahmaputra River.

61 Although a growing body of evidence has shown that WY is affected by climate, vegetation, and
62 cryosphere in the QTP, most studies have focused on individual sub-basins and have not considered these
63 three aspects together throughout this large and understudied region (Dierauer et al., 2018; Goulden and
64 Bales, 2014; Kraaijenbrink et al. 2021; Song et al., 2021; Zhou et al., 2021). Therefore, previous results
65 may not fully reveal the spatial variability in the region. Of specific interest is the Upper Brahmaputra
66 River (UBR) basin, which covers an area of over 198,636 km² (Table S1) and has large gradients in
67 elevation, climate, and vegetation (Li et al., 2019b). Therefore, providing a comprehensive, spatially
68 differentiated study of the WY changes in the UBR basin that considers the joint effects of the climate,
69 vegetation, and cryosphere is imperative. However, studies of WY changes in this region are significantly



70 hindered by the sparse network of hydrological observation stations (Li et al., 2019b; Wang L et al., 2021;
71 Yao et al., 2019), which leads to large uncertainties in WY forecasts and, thus, water resources assessments.
72 In addition, current precipitation estimates are highly uncertain owing to the complex topography of the
73 region, which limits the ability to accurately model the relationships between precipitation and runoff (Sun
74 and Su, 2020). Lastly, the present limited understanding of WY responses to the joint interaction of the
75 climate, vegetation, and cryosphere has become the biggest challenge for developing accurate physically-
76 based cryosphere-hydrological models (Pellicciotti et al., 2012). Nevertheless, long-term runoff data and
77 high-resolution satellite records of climate and vegetation cover provide a potential pathway for
78 determining their relationships using statistical methods.

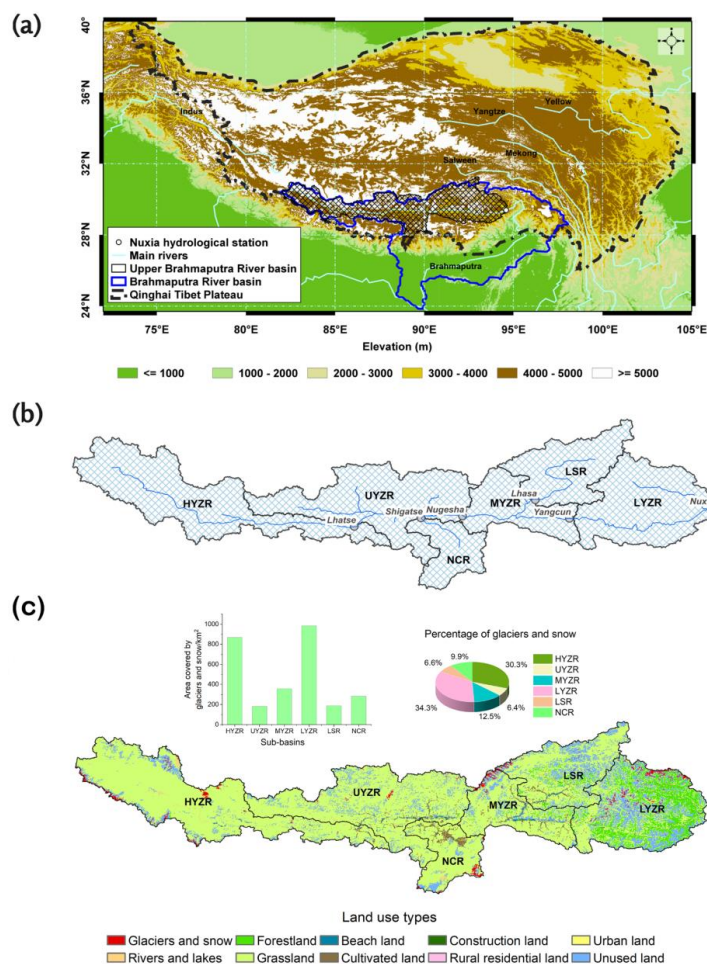
79 In this study, we collected annual runoff data for 1982–2013 from six hydrological stations to detect
80 long-term changes in the WY over the UBR basin. In addition, a modified double mass curve (DMC)
81 method was implemented to assess the influence of climate, vegetation, and the cryosphere on WY.
82 Accordingly, the main objectives of this study were to identify the magnitude and direction of changes in
83 WY based on observed runoff data and quantify the contributions of the climate, vegetation, and
84 cryosphere to these changes. This study can provide a reference for physical-based cryosphere-
85 hydrological modeling and important information for water resources and ecosystem management over the
86 UBR basin and other mountainous regions.

87 **2 Data and Methods**

88 **2.1 Study area**

89 The Brahmaputra River (known as the Yarlung Zangbo River, or YZR, in China), a transboundary river in
90 the southern QTP, originates in the Gyama Langdzom Glacier and flows across China, India, and
91 Bangladesh, before emptying into the Indian Ocean. The UBR basin is located above the Nuxia
92 hydrological station (Fig. 1a), and its flow has significant implications for the ecology of the source region
93 and freshwater resources of South Asia. Here, we divided the UBR basin into the headstream (HYZR),
94 upstream (UYZR), midstream (MYZR), downstream (LYZR), Nianchu River (NCR), and Lhasa River
95 (LSR) by hydrological stations (Fig. 1b and Table S1), and analyzed WY changes over these six sub-basins
96 to reveal spatial differences.

97 The elevation gradient and the distance to the ocean in the UBR basin together contribute to a large
98 spatial variability in the climate (Sang et al., 2016; Wang Y et al., 2020, 2021). The annual precipitation in
99 the HYZR basin is less than 400 mm, while that in the LYZR basin is nearly 1000 mm (Fig. S1). Similarly,
100 the annual actual evapotranspiration (AET) increases gradually from upstream to downstream areas (Fig.
101 S1). Meanwhile, water and energy availability modulate the vegetation conditions (Li et al., 2019a);
102 vegetation cover increases dramatically from the HYZR to the LYZR basin (Fig. S1). Furthermore, glacial
103 snow meltwater from the cryosphere due to warming conditions has substantially affected the hydrology of
104 this region (Cuo et al., 2019; Yao et al., 2010; Wang L et al., 2021).



105

106 **Figure 1.** Location of (a) the Upper Brahmaputra River (UBR) basin over the Qinghai Tibet Plateau; (b) the six sub-
 107 basins delineated by the Lhatse, Nugesha, Shigatse, Yangcun, Lhasa, and Nuxia hydrological stations; and (c) the
 108 distribution of land use types and percentage of area covered by glaciers and snow in 2015, provided by National
 109 Tibetan Plateau Data Center (<http://data.tpdc.ac.cn>).

110 2.2 Dataset

111 2.2.1 Runoff data

112 Annual runoff data between 1982 and 2013 from six hydrological stations along the mainstream and major
 113 branches, which were provided by the Hydrology and Water Resources Survey Bureau of the Tibet
 114 Autonomous Region, were used in the study. The WY in the HYZR was determined by the runoff
 115 observed at the Lhatse hydrological station, while the WY in other sub-basins was determined by the
 116 difference between runoff observed from gauging stations located at the downstream station and that at the
 117 upstream and branch stations. For example, WY in the MYZR basin was equal to the difference between
 118 the observed annual runoff in the Yangcun hydrological station and that in the Lhasa and Nugesha stations



119 (Fig. 1b).

120 **2.2.2 Climate data**

121 The most recent 10 km gridded daily precipitation dataset was obtained from Sun and Su (2020), which
122 combined topographic and linear correction approaches based on 262 rain-gauge observations, and was
123 applied to estimate regional annual precipitation (P) in this study. Regional annual AET was acquired from
124 the Global Land Evaporation Amsterdam Model (GLEAM) products with a spatial resolution of 0.25°
125 (Martens et al., 2017). The effective precipitation (eP) was regarded as a proxy for climate in this study and
126 was calculated as the difference between P and AET, as shown in Section 2.3.2.

127 **2.2.3 Vegetation data**

128 The leaf area index (LAI) data used in this study were obtained from the Global Inventory Monitoring and
129 Modelling System (GIMMS) (<https://ecocast.arc.nasa.gov/data/pub/gimms>), and spanned 1982 to 2015
130 with a spatial resolution of 8 km × 8 km. GIMMS LAI3g (Zhu et al., 2013) was generated using an
131 artificial neural network trained on the Collection Terra Moderate Resolution Imaging Spectroradiometer
132 (MODIS) LAI product and the latest version of GIMMS NDVI3g (normalized difference vegetation index)
133 data for the same period, which has been proven to have an improved multi-sensor record harmonization
134 scheme compared to other global LAI products (Forzieri et al., 2020; Gonsamo et al., 2021). Note that all
135 gridded data were aggregated to regional values over each sub-basin on an annual time scale from 1982 to
136 2013, considering area-weighted effects.

137 **2.3 Methodology**

138 **2.3.1 Trend and abrupt analysis**

139 In this study, we used the non-parametric Mann–Kendall test (Kendall, 1938; Mann, 1945) to identify the
140 trends in WY, and the non-parametric Pettitt abrupt detection method (Pettitt, 1979) to identify the turning
141 points (TP) in WY. The level of significance was set at 0.05. We compared the average WY before and
142 after each TP to reflect the magnitude of WY changes, and compared the trends before and after each TP to
143 reflect the direction of the changes.

144 **2.3.2 Double mass curve**

145 In a large and pristine mountainous river basin with diverse vegetation, climatic variability, cryospheric
146 melt, and vegetation dynamics are the three primary drivers of hydrological variation. Climatic variability
147 is typically more dominant and can often obscure the effects of other changes on hydrology (Cong et al.,
148 2009). The climatic effects on the annual WY must be excluded to enable quantification of the relative
149 contributions of the cryosphere and vegetation. According to the river basin water balance, the WY is
150 determined by the difference between precipitation, evapotranspiration, and changes in soil water storage.
151 Annual changes in soil water storage can generally be assumed to be constant and minor terms in the water
152 balance equation (Wei et al., 2009; Zhang et al., 2001); therefore, WY is mainly affected by precipitation
153 and evapotranspiration. Furthermore, precipitation has been proven to be the dominant factor for runoff
154 variation in the UBR basin (Li et al., 2019b; Wang Y et al., 2021; Xin et al., 2021). Hence, we defined the



155 difference between precipitation and evapotranspiration as eP for WY, which was used as an integrated
 156 index for climatic variability in this study.

157 Unlike the traditional DMC method, where the accumulated WY from the disturbed watershed is
 158 plotted against the accumulated WY from an undisturbed watershed, the modified DMC plots accumulated
 159 annual WY versus accumulated annual eP in the URB basin. Specifically, the modified DMC used in this
 160 study is a plot of the cumulative data of one variable versus the cumulative data of another related variable
 161 in a concurrent period. It has previously been used to assess the effects of climate (Gao et al., 2011), forest
 162 disturbance (Wei and Zhang, 2010), wildfire (Hallema et al., 2018), and the cryosphere (Brahney et al.,
 163 2017) on water resources. Here, we built two types of DMC plots to assess the effects of climate (eP),
 164 vegetation (LAI), and the cryosphere on WY changes over the entire UBR basin (which are shown in Fig.
 165 S2).

166 First, the inter-annual total WY deviation ($\Delta WY(t)$, black diamond in Fig. S2) can be calculated as the
 167 difference between WY after a TP ($WY(t)$) and the average WY before that TP ($\frac{\sum_{t=1}^{t=tp} WY(t)}{tp}$), as follows:

$$168 \quad \Delta WY(t) = WY(t) - \frac{\sum_{t=1}^{t=tp} WY(t)}{tp}, t = tp + 1, tp + 2, \dots, 32 \quad (1)$$

169 Second, the regression equation between the cumulative eP ($\sum eP$) and cumulative WY ($\sum WY$)
 170 before the TP can be constructed as follows:

$$171 \quad \sum WY = a_1 \sum eP + b_1 \quad (2)$$

172 Similarly, the regression equation between the cumulative LAI ($\sum LAI$) and cumulative WY ($\sum WY$)
 173 before the TP can be constructed as follows:

$$174 \quad \sum WY = a_2 \sum LAI + b_2 \quad (3)$$

175 Third, WY changes caused by climate change ($WY_c(t)$) can be calculated by inputting the cumulative
 176 eP after the TP into Eq. 2. Therefore, the WY deviation caused by climate change ($\Delta WY_c(t)$, blue bar in
 177 Fig. S2) can be calculated as follows:

$$178 \quad \Delta WY_c(t) = WY_c(t) - \frac{\sum_{t=1}^{t=tp} WY(t)}{tp}, t = tp + 1, tp + 2, \dots, 32 \quad (4)$$

179 Similarly, the WY changes caused by vegetation ($WY_v(t)$) were calculated using Eq. 3, and the WY
 180 deviation caused by vegetation (WY_v , tan bar in Fig. S2) can be calculated as follows:

$$181 \quad \Delta WY_v(t) = WY_v(t) - \frac{\sum_{t=1}^{t=tp} WY(t)}{tp}, t = tp + 1, tp + 2, \dots, 32 \quad (5)$$

182 Finally, the WY deviation caused by the cryosphere (ΔWY_s , red bar in Fig. S2) can be calculated as:

$$183 \quad \Delta WY_s(t) = \Delta WY(t) - \Delta WY_c(t) - \Delta WY_v(t) \quad (6)$$



184 **2.3.3 Attribution analysis on changes in water yield**

185 The average effects of climate, vegetation, and cryosphere on the magnitude of the changes in WY were
186 calculated as follows:

$$\begin{aligned} 187 \quad \overline{\Delta WY_c} &= \frac{\sum_{t=t+1}^{t=32} WY_c(t)}{32 - tp} \\ 188 \quad \overline{\Delta WY_v} &= \frac{\sum_{t=t+1}^{t=32} WY_v(t)}{32 - tp} \\ 189 \quad \overline{\Delta WY_s} &= \frac{\sum_{t=t+1}^{t=32} WY_s(t)}{32 - tp} \end{aligned} \quad (7)$$

190 The relative contribution (*RC*), ranging from 0 to 100, of climate, vegetation, and cryosphere changes
191 on the magnitude can be calculated as follows:

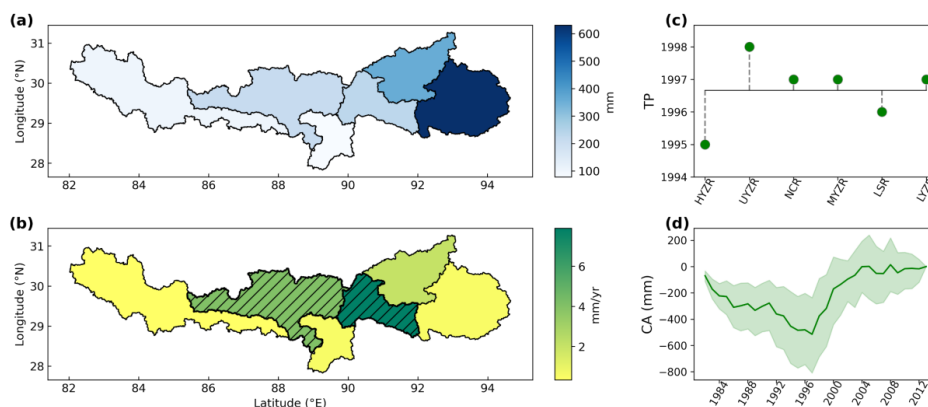
$$\begin{aligned} 192 \quad RC_c &= \frac{\overline{\Delta WY_c}}{|\overline{\Delta WY_c}| + |\overline{\Delta WY_v}| + |\overline{\Delta WY_s}|} \\ 193 \quad RC_v &= \frac{\overline{\Delta WY_v}}{|\overline{\Delta WY_c}| + |\overline{\Delta WY_v}| + |\overline{\Delta WY_s}|} \\ 194 \quad RC_s &= \frac{\overline{\Delta WY_s}}{|\overline{\Delta WY_c}| + |\overline{\Delta WY_v}| + |\overline{\Delta WY_s}|} \end{aligned} \quad (8)$$

195 In addition, we used the Pearson correlation coefficient (*r*) to quantify the relationships between the
196 total WY deviation ($\Delta WY(t)$) and its components, which were the WY deviation caused by climate
197 ($\Delta WY_c(t)$), vegetation ($\Delta WY_v(t)$), and cryosphere ($\Delta WY_s(t)$). The Student's t-test was used to detect
198 statistical significance for the Pearson's correlation coefficient at a level of 0.05.

199 **3 Results**

200 **3.1 Long-term changes in historical water yield**

201 The detection of long-term changes in WY from 1982 to 2013 over the entire UBR basin is illustrated in
202 Fig. 2. We found that there was great spatial variability in the annual WY (Fig. 2a). The mean annual WY
203 was highest in the LYZR basin (over 600 mm), followed by that over the LSR basin (nearly 400 mm).
204 However, the mean annual WY in the HYZR and NCR basins was less than 100 mm. The spatial
205 variability in annual WY was consistent with that of precipitation (Fig. S3), which was mainly determined
206 by elevation and distance to the ocean (Sang et al., 2016). WY generally increased during the study period,
207 as shown by the positive slope in Fig. 2b, which is in agreement with previous studies on a single basin (Li
208 et al., 2021; Lin et al., 2020; Zhang et al., 2011). However, a significant trend was only detected in the
209 UYZR and MYZR basins (hatched areas in Fig. 2b) in this study.



210

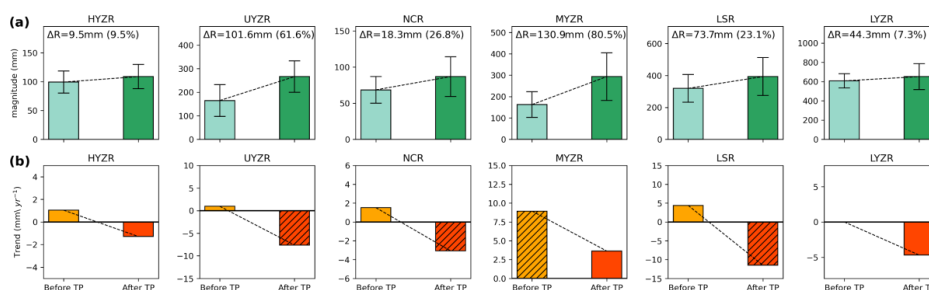
211 **Figure 2.** Long-term water yield changes over the six sub-basins, covering the entire UBR basin. (a) The mean annual
212 values by averaging water yield from 1982 to 2013. (b) The temporal variation trends detected by the Mann-Kendall
213 Sen's slope. The black hatching represents statistically significant ($p < 0.05$) trends. (c) The turning points (TP) as
214 detected by the Pettitt method. (d) The cumulative water yield anomaly (CA) curve. The solid green line represents the
215 ensemble expectation of the cumulative water yield curves for the entire UBR basin (green shading).

216 We used the Pettitt method to identify the TPs in the WY over the entire UBR basin. The TPs mainly
217 occurred during the late 1990s; however, the abrupt change detected in some sub-basins was not
218 statistically significant (Fig. 2c and Table. S2). Similarly, the cumulative anomaly curve (Fig. 2d) showed
219 that WY decreased prior to the late 1990s and then increased over the entire UBR basin, which further
220 complemented the results obtained from the Pettitt method. Our results agree with lake area changes in the
221 Tibetan Plateau (Zhang et al., 2017) and climate shifts in the UBR basin (Li et al., 2019b).

222 3.2 Regime shifts in historical water yield

223 Based on the TPs, we divided the study period from 1982 to 2013 into before and after TP periods, and
224 analyzed the magnitude and direction of the WY changes over the entire UBR basin. Figure 3 shows that
225 the WY increased from 9.5 to 130.9 mm, with high spatial variability. The slight increase observed in the
226 HYZR and LYZR basins accounted for less than 10% of the mean annual water yield before the TP.
227 Nevertheless, a substantial increase in WY of 61.6% and 80.5% was found in the UYZR and MYZR
228 basins, respectively. In addition, higher standard deviations were detected for WY after TP, suggesting
229 more dramatic variability in the entire UBR basin in later years.

230 For the direction of the WY changes, we found that the change in WY was positive before the TP but
231 became negative afterward in most sub-basins. A significant decreasing trend was detected after the TP in
232 the UYZR, NCR, and LSR basins. In contrast, although the WY in the MYZR basin increased during two
233 periods, the rate of increase had slowed, as the positive trend after the TP (3.64 mm yr^{-1} , $p > 0.05$) was less
234 than that before the TP (8.95 mm yr^{-1} , $p < 0.05$). Overall, we found that regime shifts in the WY occurred
235 in the late 1990s over the entire UBR basin; the magnitude of the WY changes generally increased, while
236 the direction of the changes reversed or slowed.



237

238 **Figure 3.** Water yield regime shifts over the entire UBR basin. **(a)** Magnitude of the water yield changes. The error bars
 239 represent the standard deviation of the water yield before (light green) and after turning point (TP) (green). **(b)**
 240 Direction of the water yield changes. The black hatching represents a statistically significant ($p < 0.05$) trend.

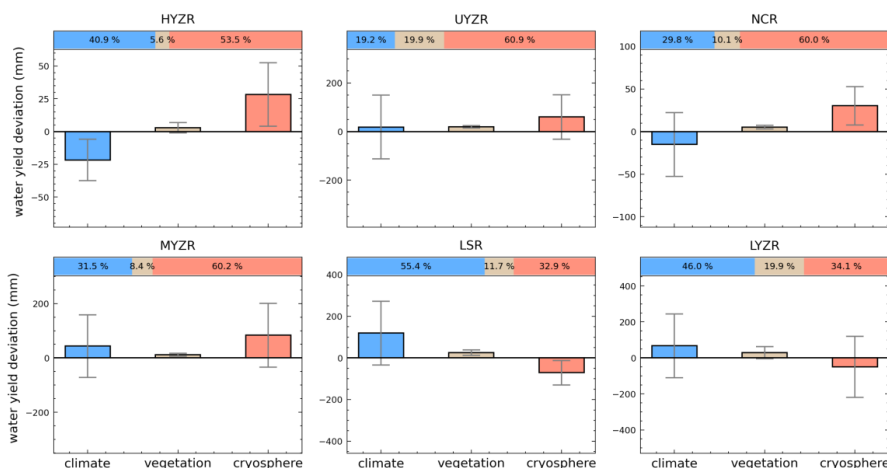
241 3.3 Attribution analysis on magnitude increases in water yield

242 As shown in Fig. 4, we quantified the contributions from climate (eP), vegetation (LAI), and the
 243 cryosphere on the WY magnitude increases over the entire UBR basin. We found that the changes in the
 244 cryosphere contributed to over half of the magnitude increases in the HYZR, UYZR, NCR, and MYZR
 245 basins. However, climate played a more important role in the magnitude increase in the LSR and LYZR
 246 basins, with relative contributions of 55.4% and 46.0%, respectively. In contrast to the dominant roles of
 247 the climate and cryosphere, vegetation had a consistently positive contribution to the magnitude increases
 248 in WY over the entire UBR basin, although the relative contributions of 5.6% in the HYZR basin and 19.9%
 249 in the LYZR basin were much less than those from the changes in the climate and cryosphere.

250 The climate and cryosphere – two important factors influencing the magnitude change in WY –
 251 together contributed over 80% to the magnitude increases over the entire UBR basin; however, they played
 252 both additive or offsetting roles (Fig. 4), resulting in slight or substantial WY increases (Fig. 3). For
 253 example, although the cryosphere change resulted in increases of 28.3 mm and 30.3 mm in the HYZR and
 254 NCR basins, the negative contributions from climate offset a considerable part of these increases resulting
 255 in the slight increase after the TP in these regions. Additionally, the positive contribution from climate
 256 offset the negative contribution from the cryosphere in the LSR and LYZR basins, which resulted in a
 257 similar slight increase in WY. However, the additive effects from the climate and cryosphere change lead
 258 to substantial increases in WY from 162.6 mm to 293.5 mm in the MYZR basin and from 164.9 mm or
 259 266.5 mm in the UYZR basin.

260

261

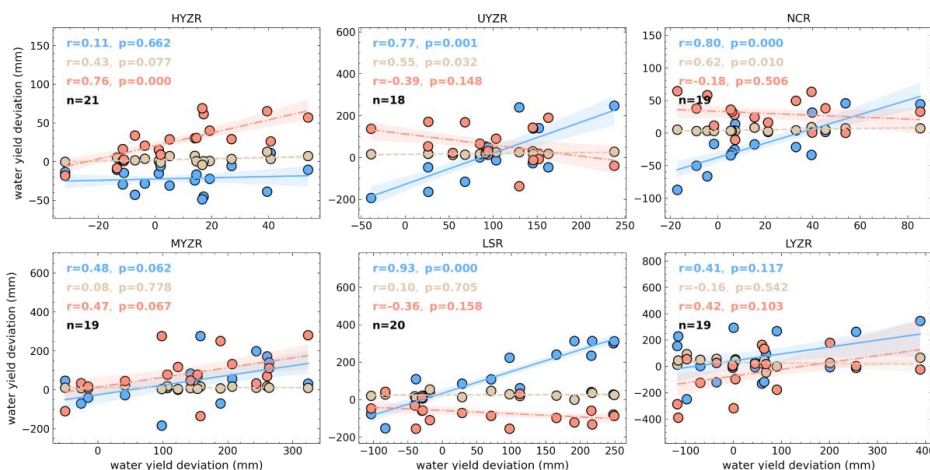


262

263 **Figure 4.** Attribution analysis of the magnitude increase in the water yield due to climate (blue bar), vegetation (tan
 264 bar), and the cryosphere (red bar), and their relative contributions (the bar on the top) in each basin. The error bars
 265 represent the standard deviation of the water yield changes caused by the various drivers (see Fig. S2).

266 **3.4 Attribution analysis on direction shifts in water yield**

267 In this study, Pearson's correlation coefficient was applied to determine the role of the climate, vegetation,
 268 and cryosphere in the reversed or slowed WY trend after the TPs, as shown in Fig. 3b. The climate played
 269 a dominant positive role in influencing the direction of the WY changes after the TP in most sub-basins
 270 (Fig. 5), which was supported by correlations ranging from 0.41 (LYZR basin) to 0.93 (LSR basin).
 271 However, the changes in WY induced by the cryosphere instead determined the decreasing trend in WY
 272 over the HYZR basin ($r = 0.76, p < 0.05$). Compared to the significantly positive role of climate, however,
 273 cryosphere-induced changes in WY in the UYZR, NCR, and LSR basins exhibited a negative correlation
 274 with the decreased WY after the TP. This suggests that meltwater from the cryosphere alleviated the loss of
 275 water resources in these regions. In addition, this effect was also detected in the MYZR basin, and together
 276 with that of climate, contributed to the increasing trend in the WY in this sub-basin. Despite the weak
 277 contribution from vegetation compared to that of the other two drivers (Fig. 4), its positive role in WY
 278 decline after the TPs was more apparent in the drier sub-basins (such as HYZR, UYZR, and NCR),
 279 whereas the correlation was negative in the humid LYZR basin.



280

281 **Figure 5.** The relationship between the time-series of the total water yield deviation ($\Delta WY(t)$, x-axis) and its
282 components (y-axis) induced by climate ($\Delta WY_c(t)$, blue point), vegetation ($\Delta WY_v(t)$, tan point), and cryosphere ($\Delta WY_s(t)$,
283 red point), respectively. The shading area indicates the 95% confidence interval of the fitting. n indicates the number of
284 years after the TP, which was determined by the Pettitt method (See Fig. 2c and Table S2).

285 4 Discussion

286 The changes in water yield can primarily be attributed to climate change and the cryosphere; nevertheless,
287 they are affected by a complex variety of factors (Harris et al., 2018; Liu et al., 2020; Peng et al. 2017),
288 such as vegetation, snow cover, permafrost, hydrology, and soil properties. Accurate monitoring of
289 cryospheric processes is essential for understanding the changing composite interactions in alpine regions
290 and predicting regional responses to climate warming (Yao et al., 2019). Although some in situ
291 observations have included more physical variables, such as soil moisture and temperature monitoring
292 networks in Naqu and Pali (Chen et al. 2017) and observations of snow and glacial melt runoff in glacier-
293 fed basins (Zhang et al. 2016), there remain large unassessed areas in the UBR basin. The harsh climate
294 and environmental conditions in these regions remain quite challenging to accurate cryosphere-
295 hydrological modeling. In this study, with the support of the Hydrology and Water Resources Survey
296 Bureau of the Tibet Autonomous Region, we collected long-term runoff-gauge data throughout the UBR,
297 examined historical water yield changes, and provided a useful alternative statistical method to physical
298 modeling approaches that can be applied to large-scale alpine river basins to quickly partition the effects of
299 climatic and cryospheric changes on the hydrological regime. Nevertheless, further numerical modeling
300 tools with coupled cryospheric and hydrospheric processes and comprehensive observational data (e.g.,
301 Wang et al. 2017) should be developed to better physically and comprehensively understand the
302 mechanisms of the runoff variations in the UBR basin.

303 Previous studies have demonstrated an increasing trend in WY over the LSR (Lin et al., 2020), LYZR
304 (Zhang et al., 2011), and UBR basins (Li et al., 2021). In this study, we provided further evidence of the
305 long-term trends in WY changes in the above regions, and, furthermore, conducted trend analysis for other
306 regions that have received less attention in the existing literature. Our results comprehensively indicated a
307 general increase in WY (Fig. 2a) over the entire UBR basin. Furthermore, we extended the duration of the



308 runoff observations to 2013 and found that regime shifts in WY occurred during the late 1990s over the
309 entire UBR basin. Moreover, the magnitude of WY increased (Fig. 3a), but the direction of WY reversed
310 or slowed after the TPs (Fig. 3b). To the best of our knowledge, these regime shifts in the WY have not
311 been reported in previous studies.

312 Our results indicated that the climate and cryosphere were important factors for magnitude increases
313 in WY throughout the UBR basin, but their relative contribution varies across regions. Climate explained a
314 greater increase in WY in downstream regions, while cryospheric changes were more important in
315 upstream regions (Fig. 4); this matches the relative importance of meltwater from the cryosphere to
316 streamflow (Fig. S4). According to Biemans et al. (2019), meltwater from the cryosphere is the most
317 important water source in the upper regions of the Indo-Gangetic Plain, supplying over 40% of the total
318 WY upstream but less than 30% downstream. The effect of vegetation on changes on WY was much less
319 than that of the climate and cryosphere (Fig. 4 and Fig. S2). Additionally, offsetting or additive effects
320 from climate and cryosphere changes were detected in this study (Fig. 4), which led to either slight or
321 substantial increase in WY in each region of the UBR basin (Fig. 3a). The additive effect is beneficial for
322 mitigating drought, but it could exacerbate the flood risks due to increased precipitation and accelerated
323 melting of the cryosphere in the future (Immerzeel et al., 2013). More importantly, the combined effects
324 often hinder the roles of each driver in hydrological changes, which should be considered when designing
325 water management strategies and ecological restoration engineering (Wei et al., 2018; Zhang and Wei,
326 2021).

327 Although climate and cryosphere together contributed to the magnitude increases in WY throughout
328 the UBR basin, climate remained the most important factor controlling the declining WY in most regions
329 (Fig. 5). Simultaneously, significant cryosphere changes due to global warming influenced the direction of
330 the WY changes, which is supported by glacier retraction (Yao et al., 2010) and several modeling studies
331 (Lutz et al., 2014; Zhang et al., 2020; Wang Y et al., 2021). Similarly, our study indicated that meltwater
332 from cryospheric changes has the potential to alleviate reduced water resources in most regions (Fig. 3b).
333 However, in the HYZR basin, the decline in cryosphere-induced WY became a more important driver of
334 the decreasing WY trend after the TP, which was inferred from the strong positive correlation ($r = 0.76$, p
335 < 0.05 , Fig. 5). The meltwater from snow and glaciers in the cryosphere accounted for over 60% of the
336 streamflow in the HYZR basin (Biemans et al., 2019) and was critical for regional ecology; however, our
337 statistical results suggested a decreasing supply from the cryosphere after the TP in the HYZR basin, which
338 could be important for ecological restoration in river sources and emphasizes more explicit physical-based
339 cryosphere–hydrology modeling.

340 Effective precipitation, an integrated climatic index that was generated by subtracting the actual
341 evapotranspiration from the precipitation, was used in the DMC method. As shown in Fig. S3, the mean
342 annual WY of all six sub-basins showed a consistently linear relationship with the corresponding mean
343 annual precipitation, further proving the dominant role of precipitation in the spatial and temporal
344 characteristics of the WY throughout the UBR basin. In addition, Wei et al. (2010, 2018) and Zheng et al.
345 (2009) conducted attribution analyses of the streamflow caused by climate and land surface changes in
346 large-scale river basins with mountains and diverse vegetation; they indicated that streamflow variation and
347 climate variability show a linear relationship, which provides solid evidence for the assumption of a linear



348 relationship between the WY variation and effective precipitation in the present study. Furthermore, the
349 results prove that the effects of climate variability could be successfully separated to present a clearer
350 picture of the cumulative and annual effects of the cryosphere and vegetation changes on the WY in the
351 UBR basin.

352 **5 Conclusions**

353 In this study, regime shifts in WY were detected during the late 1990s over the UBR basin. The magnitude
354 of the WY generally increased, but its direction reversed or slowed. We used the DMC method to assess
355 the effects of the climate, vegetation, and cryosphere on the WY and found that the changes in the climate
356 and cryosphere had either an offsetting or additive effect, which caused either a slight or substantial
357 increase in the WY, whereas the role of vegetation was much smaller. Furthermore, the declining or
358 slowing WY after the TPs was mainly driven by climate in most regions, and notably, meltwater from the
359 cryosphere had the potential to alleviate reduced water resources. These findings suggest that the combined
360 effects of the climate and cryosphere should be considered in the sustainable development of water
361 resources and ecosystems, especially the co-benefits in upstream and downstream regions.

362 *Data availability.* The datasets generated for this study are available on request to the corresponding author.

363 *Author contributions.* HL: conceptualisation, data curation, formal analysis, methodology, writing –
364 original draft, writing – review and editing. LL: conceptualisation, formal analysis, methodology, writing –
365 review and editing, funding acquisition. BYS: data curation, methodology. LW: supervision, writing –
366 review and editing. AK: validation, writing – review and editing. FZ&DFL: software, validation. XXW:
367 visualization. WFL&XPL: Writing – review & editing. ZXX: supervision, resources.

368 *Competing interests.* The contact author has declared that neither they nor their co-authors have any
369 competing interests.

370 *Acknowledgments.* This work was jointly supported by the National Natural Science Foundation of China
371 (Grant No. 51961145104, 52079138, and 91647202), the 2115 Talent Development Program of China
372 Agricultural University (00109019), and the China Scholarship Council (Grant No. 202006350051). Hao
373 Li thanks the China Scholarship Council (CSC) for providing financial support to pursue his PhD in
374 Belgium.



375 **References**

- 376 Bibi, S., Wang, L., Li, X., Zhou, J., Chen, D., and Yao, T.: Climatic and associated cryospheric, biospheric,
377 and hydrological changes on the Tibetan Plateau: A review, *Int. J. Climatol.*, 38, e1–e17,
378 <https://doi.org/10.1002/joc.5411>, 2018.
- 379 Biemans, H., Siderius, C., Lutz, A., Nepal, S., Ahmad, B., Hassan, T., von Bloh, W., Wijngaard, R.,
380 Wester, P., Shrestha, A., and Immerzeel, W. W.: Importance of snow and glacier meltwater for
381 agriculture on the Indo-Gangetic Plain, *Nat Sustain.*, 2, 594–601, [https://doi.org/10.1038/s41893-019-](https://doi.org/10.1038/s41893-019-0305-3)
382 0305-3, 2019.
- 383 Brahney, J., Menounos, B., Wei, X., and Curtis, P. J.: Determining annual cryosphere storage contributions
384 to streamflow using historical hydrometric records, *Hydrol. Process.*, 31, 1590–1601,
385 <https://doi.org/10.1002/hyp.11128>, 2017.
- 386 Chen, Y., Yang, K., Qin, J., Cui, Q., Lu, H., La, Z., Han, M., and Tang, W.: Evaluation of SMAP, SMOS,
387 and AMSR2 soil moisture retrievals against observations from two networks on the Tibetan Plateau, *J.*
388 *Geophys. Res.: Atmos.*, 122, 5780–5792, <https://doi.org/10.1002/2016JD026388>, 2017.
- 389 Cong, Z., Yang, D., Gao, B., Yang, H., and Hu, H.: Hydrological trend analysis in the Yellow River basin
390 using a distributed hydrological model, *Water. Resour. Res.*, 45, W00A13, doi:10.1029/2008WR006852,
391 2009.
- 392 Cuo, L., Li, N., Liu, Z., Ding, J., Liang, L., Zhang, Y., and Gong, T.: Warming and human activities
393 induced changes in the Yarlung Tsangpo basin of the Tibetan Plateau and their influences on streamflow,
394 *J. Hydrol.: Reg. Stud.*, 25, 100625, <https://doi.org/10.1016/j.ejrh.2019.100625>, 2019.
- 395 Dierauer, J. R., Whitfield, P. H., and Allen, D. M.: Climate controls on runoff and low flows in mountain
396 catchments of western North America, *Water. Resour. Res.*, 54, 7495–7510,
397 <https://doi.org/10.1029/2018wr023087>, 2018.
- 398 Fan, H. and He, D.: Temperature and precipitation variability and its effects on streamflow in the upstream
399 regions of the Lancang–Mekong and Nu–Salween Rivers, *J. Hydrometeorol.*, 16, 2248–2263,
400 <https://doi.org/10.1175/jhm-d-14-0238.1>, 2015.
- 401 Forzieri, G., Miralles, D. G., Ciais, P., Alkama, R., Ryu, Y., Duveiller, G., Zhang, K., Robertson, E., Kautz,
402 M., Martens, B., Jiang, C. Y., Arneth, A., Georgievski, G., Li, W., Ceccherini, G., Anthoni, P.,
403 Lawrence, P., Wiltshire, A., Pongratz, J., Piao, S. L., Sitch, S., Goll, D. S., Arora, V. K., Lienert, S.,
404 Lombardozzi, D., Kato, E., Nabel, J. E. M. S., Tian, H. Q., Friedlingstein, P., and Cescatti, A.: Increased
405 control of vegetation on global terrestrial energy fluxes, *Nat. Clim. Change*, 10, 356–362,
406 <https://doi.org/10.1038/s41558-020-0717-0>, 2020.
- 407 Gao, P., Mu, X. M., Wang, F., and Li, R.: Changes in streamflow and sediment discharge and the response
408 to human activities in the middle reaches of the Yellow River, *Hydrol. Earth Syst. Sci.*, 15, 1–10,
409 <https://doi.org/10.5194/hess-15-1-2011>, 2011.
- 410 Gonsamo, A., Ciais, P., Miralles, D. G., Sitch, S., Dorigo, W., Lombardozzi, D., Friedlingstein, P., Nabel, J.
411 E., Goll, D. S., O’Sullivan, M., Arneth, A., Anthoni, P., Jain, A. K., Wiltshire, A., Peylin, P., and
412 Cescatti, A.: Greening drylands despite warming consistent with carbon dioxide fertilization effect,



- 413 Global Change Biol., 27, 3336–3349, <https://doi.org/10.1111/gcb.15658>, 2021.
- 414 Goulden, M. L. and Bales, R. C.: Mountain runoff vulnerability to increased evapotranspiration with
415 vegetation expansion, P. Natl. Acad. Sci. USA, 111, 14071–14075,
416 <https://doi.org/10.1073/pnas.1319316111>, 2014.
- 417 Hallema, D. W., Sun, G., Caldwell, P. V., Norman, S. P., Cohen, E. C., Liu, Y., Bladon, K. D., and
418 McNulty, S. G.: Burned forests impact water supplies, Nat. Commun., 9, 1–8,
419 <https://doi.org/10.1038/s41467-018-03735-6>, 2018.
- 420 Harris, S., Brouchkov, A., and Guodong, C.: Geocryology: an introduction to frozen ground, CRC Press,
421 pp 1–8, 2018.
- 422 Immerzeel, W. W., Pellicciotti, F., and Bierkens, M. F. P.: Rising river flows throughout the twenty-first
423 century in two himalayan glacierized watersheds, Nat. Geosci., 6, 742–745,
424 <https://doi.org/10.1126/science.1183188>, 2013.
- 425 Immerzeel, W. W., Van Beek, L. P., and Bierkens, M. F.: Climate change will affect the Asian water
426 towers, Science, 328, 1382–1385, <https://doi.org/10.1038/ngeo1896>, 2010.
- 427 Kang, S., Xu, Y., You, Q., Flügel, W. A., Pepin, N., and Yao, T.: Review of climate and cryospheric
428 change in the Tibetan Plateau, Environ. Res. Lett., 5, 015101, <https://doi.org/10.1088/1748-9326/5/1/015101>, 2010.
- 430 Kendall, M. G.: A new measure of rank correlation. Biometrika, 30, 81–93,
431 <https://doi.org/10.2307/2332226>, 1938.
- 432 Kraaijenbrink, P. D., Stigter, E. E., Yao, T., and Immerzeel, W. W.: Climate change decisive for Asia's
433 snow meltwater supply. Nat. Clim. Change, 11, 591–597, <https://doi.org/10.1038/s41558-021-01074-x>,
434 2021.
- 435 Li, D., Li, Z., Zhou, Y., and Lu, X.: Substantial increases in the water and sediment fluxes in the headwater
436 region of the Tibetan Plateau in response to global warming, Geophys. Res. Lett., 47, e2020GL087745,
437 <https://doi.org/10.1029/2020gl087745>, 2020.
- 438 Li, H., Liu, L., Koppa, A., Shan, B., Liu, X., Li, X., Niu, Q., Cheng, L., and Miralles, D.: Vegetation
439 greening concurs with increases in dry season water yield over the Upper Brahmaputra River basin, J.
440 Hydrol., 603, 126–981, <https://doi.org/10.1016/j.jhydrol.2021.126981>, 2021.
- 441 Li, H., Liu, L., Liu, X., Li, X., and Xu, Z.: Greening implication inferred from vegetation dynamics
442 interacted with climate change and human activities over the southeast Qinghai–Tibet Plateau, Remote
443 Sens., 11, 2421, <https://doi.org/10.3390/rs11202421>, 2019a.
- 444 Li, H., Liu, L., Shan, B., Xu, Z., Niu, Q., Cheng, L., Liu, X., and Xu, Z.: Spatiotemporal variation of
445 drought and associated multi-scale response to climate change over the Yarlung Zangbo River basin of
446 Qinghai–Tibet Plateau, China, Remote Sens., 11, 1596, <https://doi.org/10.3390/rs11131596>, 2019b.
- 447 Li, J., Liu, D., Wang, T., Li, Y., Wang, S., Yang, Y., Wang, X., Guo, H., Peng, S., Ding, J., Shen, M. G.,
448 and Wang, L.: Grassland restoration reduces water yield in the headstream region of Yangtze River, Sci.
449 Rep., 7, 1–9, <https://doi.org/10.1038/s41598-017-02413-9>, 2017.
- 450 Lin, L., Gao, M., Liu, J., Wang, J., Wang, S., Chen, X., and Liu, H.: Understanding the effects of climate
451 warming on streamflow and active groundwater storage in an alpine catchment: the upper Lhasa River.
452 Hydrol. Earth Syst. Sci., 24, 1145–1157, <https://doi.org/10.5194/hess-24-1145-2020>, 2020.



- 453 Liu, L., Luo D., Wang L., Huang Y., and Chen F.: Dynamics of freezing/thawing indices and frozen
454 ground from 1900 to 2017 in the upper Brahmaputra River Basin, Tibetan Plateau. *Adv. Clim. Chang.*
455 *Res.*, 12, 6–17, <https://doi.org/10.1016/j.accre.2020.10.003>, 2021.
- 456 Liu, L., Luo, D., Wang, L., Huang, Y., and Chen, F.: Variability of soil freeze depth in association with
457 climate change from 1901 to 2016 in the upper Brahmaputra River Basin, Tibetan Plateau, *Theor. Appl.*
458 *Climatol.*, 142, 19–28, <https://doi.org/10.1007/s00704-020-03291-4>, 2020.
- 459 Lutz, A., Immerzeel, W., Shrestha, A., and Bierkens, M.: Consistent increase in high Asia’s runoff due to
460 increasing glacier melt and precipitation, *Nat. Clim. Change*, 4, 587–592.
461 <https://doi.org/10.1038/nclimate2237>, 2014.
- 462 Mann, H. B.: Nonparametric tests against trend, *Econometrica*, 245–259, <https://doi.org/10.2307/1907187>,
463 1945.
- 464 Martens, B., Miralles, D. G., Lievens, H., Van Der Schalie, R., De Jeu, R. A., Fern’andez-Prieto, D., Beck,
465 H. E., Dorigo, W. A., and Verhoest, N. E.: GLEAM v3: Satellite-based land evaporation and root-zone
466 soil moisture, *Geosci. Model Dev.*, 10, 1903–1925, <https://doi.org/10.5194/gmd-10-1903-2017>, 2017.
- 467 Pellicciotti, F., Buergi, C., Immerzeel, W. W., Konz, M., and Shrestha, A. B.: Challenges and uncertainties
468 in hydrological modeling of remote Hindu Kush–Karakoram–Himalayan (HKH) basins: suggestions for
469 calibration strategies, *Mt. Res. Dev.*, 32, 39–50, <https://doi.org/10.1659/mrd-journal-d-11-00092.1>, 2012.
- 470 Pettitt, A. N.: A non-parametric approach to the change-point problem, *J. R. Stat. Soc. C-Appl.*, 28, 126–
471 135, <https://doi.org/10.2307/2346729>, 1979.
- 472 Sang, Y. F., Singh, V. P., Gong, T., Xu, K., Sun, F., Liu, C., Liu, W., and Chen, R.: Precipitation variability
473 and response to changing climatic condition in the Yarlung Tsangpo River basin, China. *J. Geophys.*
474 *Res.: Atmos.*, 121, 8820–8831, <https://doi.org/10.1002/2016jd025370>, 2016.
- 475 Song, C., Wang, G., Sun, X., and Hu, Z.: River runoff components change variably and respond differently
476 to climate change in the Eurasian Arctic and Qinghai-Tibet Plateau permafrost regions, *J. Hydrol.*, 601,
477 126653, <https://doi.org/10.1016/j.jhydrol.2021.126653>, 2021.
- 478 Sun, H. and Su, F.: Precipitation correction and reconstruction for streamflow simulation based on 262 rain
479 gauges in the upper Brahmaputra of southern Tibetan Plateau, *J. Hydrol.*, 590, 125484,
480 <https://doi.org/10.1016/j.jhydrol.2020.125484>, 2020.
- 481 Tang, Q., Lan, C., Su, F., Liu, X., Sun, H., Ding, J., Wang, L., Leng, G., Zhang, Y., Sang, Y., Fang, H.,
482 Zhang, S., Han, D., Liu, X., He, L., Xu, X., Tang, Y., and Chen, D. L.: Streamflow change on the
483 Qinghai-Tibet Plateau and its impacts, *Chin. Sci. Bull.*, 64, 2807–2821, <https://doi.org/10.1360/tb-2019-0141>, 2019.
- 485 Viviroli, D., Archer, D. R., Buytaert, W., Fowler, H. J., Greenwood, G. B., Hamlet, A. F., Huang, Y.,
486 Koboltschnig, G., Litaor, M., L’opez-Moreno, J. I., Lorentz, S., Schädler, B., Schreier, H., Schwaiger,
487 K., Vuille, M., and Woods, R.: Climate change and mountain water resources: overview and
488 recommendations for research, management and policy, *Hydrol. Earth Syst. Sci.*, 15, 471–504,
489 <https://doi.org/10.5194/hess-15-471-2011>, 2011.
- 490 Wang, L., Yao, T., Chai, C., Cuo, L., Su, F., Zhang, F., Yao, Z., Zhang, Y., Li, X., Qi, J., Hu, Z., Liu, J.,
491 and Wang, Y.: TP-River: Monitoring and quantifying total river runoff from the Third Pole, *B. Am.*
492 *Meteorol. Soc.*, 102(5), E948-E965, <https://doi.org/10.1175/BAMS-D-20-0207.1>, 2021.



- 493 Wang, L., Zhou, J., Qi, J., Sun, L., Yang, K., Tian, L., Lin, Y., Liu, W., Shrestha, M., Xue, Y., Koike, T.,
494 Ma, Y., Li, X., Chen, Y., Chen, D., Piao, S., and Lu, H.: Development of a land surface model with
495 coupled snow and frozen soil physics, *Water Resour. Res.*, 53, 5085–5103,
496 doi:10.1002/2017WR020451, 2017.
- 497 Wang, Y., Wang, L., Li, X., Zhou, J., and Hu, Z.: An integration of gauge, satellite and reanalysis
498 precipitation datasets for the largest river basin of the Tibetan Plateau, *Earth Syst. Sci. Data*, 12, 1789–
499 1803, <https://doi.org/10.5194/essd-12-1789-2020>, 2020.
- 500 Wang, Y., Wang, L., Zhou, J., Yao, T., Yang, W., Zhong, X., Liu, R., Hu, Z., Luo, L., Ye, Q., Chen, N.,
501 and Ding, H.: Vanishing glaciers at southeast Tibetan Plateau have not offset the declining runoff at
502 Yarlung Zangbo. *Geophys. Res. Lett.*, 48, e2021GL094651, <https://doi.org/10.1029/2021GL094651>,
503 2021.
- 504 Wei, X., Li, Q., Zhang, M., Giles-Hansen, K., Liu, W., Fan, H., Wang, Y., Zhou, G., Piao, S., and Liu, S.:
505 Vegetation cover—another dominant factor in determining global water resources in forested regions,
506 *Global Change Biol.*, 24, 786–795, <https://doi.org/10.1111/gcb.13983>, 2018.
- 507 Wei, X. and Zhang, M.: Quantifying streamflow change caused by forest disturbance at a large spatial
508 scale: A single watershed study. *Water Resour. Res.*, 46, W12525,
509 <https://doi.org/10.1029/2010wr009250>, 2010.
- 510 Xin, J., Sun, X., Liu, L., Li, H., Liu, X., Li, X., Cheng, L., and Xu, Z.: Quantifying the contribution of
511 climate and underlying surface changes to alpine runoff alterations associated with glacier melting,
512 *Hydrol. Process.*, 35, e14069, <https://doi.org/10.1002/hyp.14069>, 2021.
- 513 Yao, T., Li, Z., Yang, W., Guo, X., Zhu, L., Kang, S., Wu, Y., and Yu, W.: Glacial distribution and mass
514 balance in the Yarlung Zangbo River and its influence on lakes. *Chin. Sci. Bull.*, 55, 2072–2078,
515 <https://doi.org/10.1007/s11434-010-3213-5>, 2010.
- 516 Yao, T., Xue, Y., Chen, D., Chen, F., Thompson, L., Cui, P., Koike, T., Lau, W., Lettenmaier, D.,
517 Mosbrugger, V., Zhang, R., Xu, B., Dozier, J., Gillespie, T., Gu, X., Kang, S., Piao, S., Sugimoto, S.,
518 Ueno, K., Wang, L., Wang, W., Zhang, F., Sheng, Y., Guo, W., Ailikun, Yang, X., Ma, Y., Shen, S. S.
519 P., Su, Z., Chen, F., Liang, S., Liu, Y., Singh, V., Yang, K., Yang, D., Zhao, X., Qian, Y., Zhang, Y.,
520 and Li, Q.: Recent Third Pole’s rapid warming accompanies cryospheric melt and water cycle
521 intensification and interactions between monsoon and environment: Multidisciplinary approach with
522 observations, modeling, and analysis, *B. Am. Meteorol. Soc.*, 100, 423–444,
523 <https://doi.org/10.1175/BAMS-D-17-0057.1>, 2019.
- 524 Zhang, G., Kang, S., Cuo, L., and Qu, B.: Modeling hydrological process in a glacier basin on the central
525 Tibetan Plateau with a distributed hydrology soil vegetation model. *J. Geophys. Res.: Atmos.*, 121,
526 9521–9539, <https://doi.org/10.1002/2016JD025434>, 2016.
- 527 Zhang, G., Yao, T., Piao, S., Bolch, T., Xie, H., Chen, D., Gao, Y., O’Reilly, C. M., Shum, C. K., Yang, K.,
528 Yi, S., Lei, Y., Wang, W., He, Y., Shang, K., Yang, X., and Zhang, H.: Extensive and drastically
529 different alpine lake changes on Asia’s high plateaus during the past four decades, *Geophys. Res. Lett.*,
530 44, 252–260, <https://doi.org/10.1002/2016gl072033>, 2017.
- 531 Zhang, L., Dawes, W., and Walker, G.: Response of mean annual evapotranspiration to vegetation changes
532 at catchment scale, *Water Resour. Res.*, 37, 701–708, doi:10.1029/2000WR900325, 2001.



- 533 Zhang, M., Ren, Q., Wei, X., Wang, J., Yang, X., and Jiang, Z.: Climate change, glacier melting and
534 streamflow in the Niyang River basin, southeast Tibet, China. *Ecohydrology*, 4, 288–298,
535 <https://doi.org/10.1002/eco.206>, 2011.
- 536 Zhang, M. and Wei, X.: Deforestation, forestation, and water supply, *Science*, 371, 990–991,
537 <https://doi.org/10.1126/science.abe7821>, 2021.
- 538 Zhang, Y., Xu, C.Y., Hao, Z., Zhang, L., Ju, Q., and Lai, X.: Variation of melt water and rainfall runoff and
539 their impacts on streamflow changes during recent decades in two Tibetan Plateau basins, *Water*, 12,
540 3112, <https://doi.org/10.3390/w12113112>, 2020.
- 541 Zheng, H., Zhang, L., Zhu, R., Liu, C., Sato, Y., and Fukushima, Y.: Responses of streamflow to climate
542 and land surface change in the headwaters of the Yellow River Basin, *Water Resour. Res.*, 45, W00A19,
543 [doi:10.1029/2007WR006665](https://doi.org/10.1029/2007WR006665), 2009.
- 544 Zhou, X., Zhang, Y., Beck, H. E., and Yang, Y.: Divergent negative spring vegetation and summer runoff
545 patterns and their driving mechanisms in natural ecosystems of northern latitudes, *J. Hydrol.*, 592,
546 125848, <https://doi.org/10.1016/j.jhydrol.2020.125848>, 2021.
- 547 Zhu, Z., Bi, J., Pan, Y., Ganguly, S., Anav, A., Xu, L., Samanta, A., Piao, S., Nemani, R.R., and Myneni, R.
548 B.: Global data sets of vegetation leaf area index (LAI)_{3g} and fraction of photosynthetically active
549 radiation (FPAR)_{3g} derived from global inventory modeling and mapping studies (GIMMS) normalized
550 difference vegetation index (NDVI_{3g}) for the period 1981 to 2011. *Remote Sens.*, 5, 927–948,
551 <https://doi.org/10.3390/rs5020927>, 2013.